

## Dimensional crossover in the low-temperature transport properties of annealed amorphous Fe/Si multilayers

Yeong Kuo Lin, T. Novet, and D. C. Johnson

*Materials Science Institute, University of Oregon, Eugene, Oregon 97403*

J. M. Valles, Jr.

*Department of Physics, Brown University, Providence, Rhode Island 02912*

(Received 26 May 1993; revised manuscript received 3 August 1993)

We present measurements of the low-temperature,  $T < 20$  K, conductance,  $G(T)$ , of amorphous Fe/Si multilayers as a function of the temperature at which they are annealed,  $T_{\text{ann}}$ . We concentrate on two of the multilayers which have 10 Å thick Fe layers and different Si layer thicknesses (32 and 40 Å). At low temperatures, the quantum corrections to  $G(T)$  are logarithmic indicating that the individual Fe layers are in the two dimensional limit and are not coupled to one another. Annealing the samples at temperatures as low as 150 °C drives the interdiffusion of the Fe and Si layers. This interdiffusion leads to stronger coupling between the conducting layers and a reduction in their conductances. After an anneal at 350 °C, the conductance of the multilayer sample with the thinner Si layers rises sharply and  $G(T)$  acquires a square-root temperature dependence. This behavior signals a crossover from two to three dimensional electronic transport.

### I. INTRODUCTION

Much experimental work has shown that the conductivity of metallic systems in which the impurity scattering rate is high decreases at low temperatures. In many bulk systems the conductivity decreases with the square root of the temperature  $T$  and in very thin films it decreases as the logarithm of the temperature.<sup>1-3</sup> This behavior cannot be explained by simple Drude-like models of transport. Rather, models that explicitly include the wave nature of the conduction electrons predict “quantum corrections” to the transport that have these forms.<sup>1-3</sup>

Two types of physical effects that contribute to these quantum corrections have been identified in the weakly disordered limit  $k_F \ell > 1$ , where  $k_F$  is the Fermi wave vector and  $\ell$  is the elastic mean free path. The first are weak localization (WL) effects that are a consequence of phase coherent multiple scattering processes. These effects reduce the electronic mobility and are very sensitive to scattering processes that break the phase coherence of the electron wave functions.<sup>3</sup> The second are electron-electron ( $e-e$ ) interaction effects which arise from the enhancement of correlations between the conduction electrons and the reduction of their screening capabilities with increasing impurity scattering rate. These many body effects reduce the density of electronic states near the Fermi energy  $E_F$ .<sup>1</sup> Since the conductivity is directly proportional to the mobility and the density of states at  $E_F$  these two effects act to degrade it. In the strongly disordered limit  $k_F \ell \simeq 1$ , where the theoretical picture is not so clear, experiments suggest that these two physical effects seem to predominate right up to the metal to insulator transition.<sup>2,4</sup>

As shown experimentally and accounted for theoretically, the quantum corrections depend on the dimension-

ality of the electronic system.<sup>2</sup> Multilayers of disordered metals and insulators have been employed to explore these effects.<sup>5-7</sup> The basic idea of these experiments was to vary the thickness of the insulating layers and thus, the electronic interlayer coupling, and investigate the ensuing changes in the electronic transport. Crossovers from a two to a three dimensional dependence of the quantum corrections to the conductance have been observed as the insulator layer thicknesses were decreased.<sup>5-7</sup> We present data that show that a similar dimensional crossover occurs in FeSi multilayer films as they are thermally annealed. The annealing leads to the interdiffusion of the Fe and Si layers which increases the coupling between the conducting (i.e., higher Fe concentration) layers. The sheet resistance per layer of the multilayers that we have studied are high,  $R > 2$  kΩ, and, as a result, the signature of the crossover is particularly striking.

The remainder of this paper is organized as follows. In Sec. II we describe the preparation of the two multilayer samples and one single layer sample used in these studies, the thermal annealing processes, and our measurement techniques. We briefly review the theoretical predictions for the quantum corrections to the conductivity in Sec. III. Sections IV and V contain our results and a discussion of them, respectively, and Sec. VI serves as a summary.

### II. SAMPLES AND EXPERIMENTAL TECHNIQUES

The Fe/Si multilayers were formed by alternate electron beam evaporations of these elements onto polished silicon substrates. During deposition the substrates were kept at  $T < 80$  °C and the ambient pressure in the cham-

ber was  $\sim 7 \times 10^{-8}$  torr. The deposition amounts and rates ( $0.5 \text{ \AA}/\text{sec}$ ) were monitored with quartz microbalances. Grazing angle x-ray diffraction measurements were used to calibrate the microbalances and provide us with the measurements of the individual layer thicknesses. High angle x-ray diffraction measurements indicated that the as-deposited and thermally annealed films had amorphous structures. Further details about the deposition methods and x-ray techniques are discussed in Ref. 8. The two samples on which we concentrate here consisted of 20 alternating layers of  $10 \text{ \AA}$  of Fe and  $32 \text{ \AA}$  of Si (sample 1) and  $10 \text{ \AA}$  of Fe and  $40 \text{ \AA}$  of Si (sample 2). The total concentrations of Fe in samples 1 and 2 were 30% and 35%, respectively. In addition, we will compare data from the multilayers with data from a single layer sample of A:B:A structure ( $20 \text{ \AA}$  Si:  $10 \text{ \AA}$  Fe:  $20 \text{ \AA}$  Si) in order to determine which of the observed properties depend explicitly on the multilayer structure.

The low-temperature transport properties of disordered metals are sensitive to the presence of magnetic fields and magnetic impurities that can spin-flip or skew-scatter conduction electrons.<sup>3,9</sup> It is therefore important to have a picture of the magnetic properties of our films. For ease of discussion we refer to an idealized picture of the Fe concentration profile as a function of position for a portion of a multilayer in Fig. 1. The profiles are qualitatively consistent with our x-ray measurements. The unannealed curve corresponds to the as-deposited film. In the as-deposited state, we assert that the central portions of the Fe layers are ferromagnetic even though their total layer thicknesses are only  $10 \text{ \AA}$ . This is supported by the fact that we have observed an anomalous contribution to the Hall coefficient that saturates in high magnetic fields.<sup>10</sup> This indicates that the magnetization of the Fe layers saturates as it would in an amorphous ferromagnet. In addition, it is likely that the interfaces between the Fe and Si layers are probably nonmagnetic. Our low angle x-ray studies show that there is a mixing

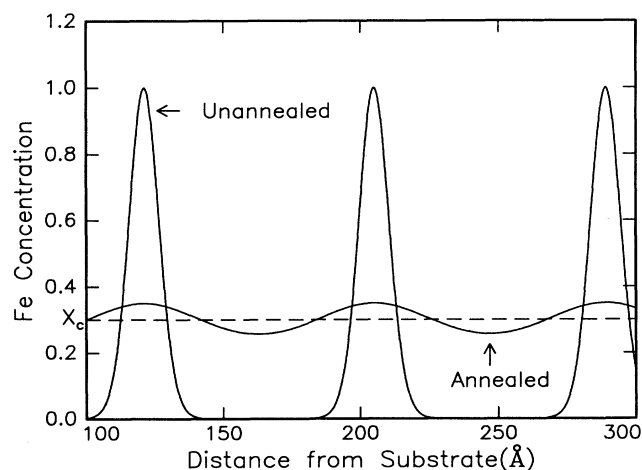


FIG. 1. Schematic profiles of the Fe concentration for an unannealed and an annealed sample as a function of the distance from the substrate.  $x_c$  is an estimate of the critical concentration for the metal-insulator transition in bulk  $\text{Fe}_x\text{Si}_{1-x}$ .

of the Fe and Si at the interfaces that extends over about  $6 \text{ \AA}$ .<sup>8</sup> If the Fe and Si mixture in this region behaves like bulk amorphous composites  $\text{Fe}_x\text{Si}_{1-x}$ , for which ferromagnetism disappears for  $x < 0.4$ ,<sup>11</sup> then we expect a significant portion of the interface region to be nonmagnetic. Mossbauer spectroscopy studies<sup>12,13</sup> of similar Fe/Si multilayers are in good agreement with this overall picture.

The intensity of the low angle x-ray peaks which result from the superlattice structure was used to determine the amplitude of the spatial modulation of the Fe concentration through the multilayers. Our x-ray results show that annealing these multilayers has the qualitative effect on their structure shown in Fig. 1. That is, the amplitude of the spatial modulation of the Fe concentration decreases. This indicates that the Fe and Si layers interdiffuse at elevated temperatures. The highest temperature annealing steps reduced the modulation of the Fe concentration relative to the unannealed modulation by a factor of 10 in sample 1, and a factor of 6 in sample 2. This implies that the thinner Si layers allow a more homogeneous composite to form.

The annealing steps were carried out in an oxygen-free dry box at temperatures in the range  $150^\circ\text{C} < T_{\text{ann}} < 400^\circ\text{C}$  for 9 to 12 h. We estimate our annealing temperature uncertainty to be  $10^\circ\text{C}$ . Differential scanning calorimetry measurements on similar multilayers indicated that they react to thermal annealing in two steps. As shown in Fig. 2 there is a broad low-temperature exotherm and a sharp high temperature exotherm. High angle x-ray diffraction measurements and transmission electron microscopy measurements showed that the multilayers remained amorphous for annealing temperatures

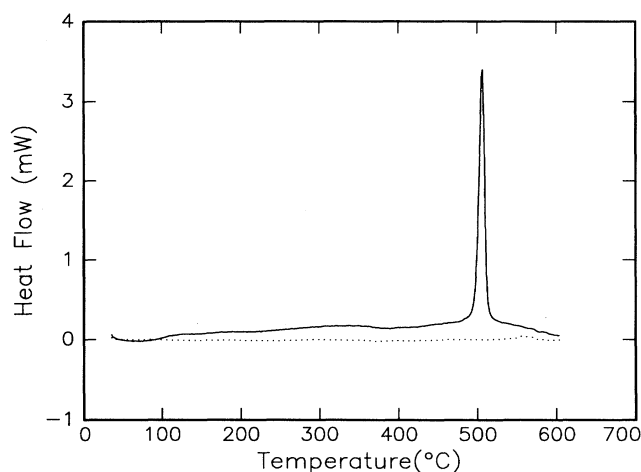


FIG. 2. The heat flow rate from an Fe/Si multilayer composed of  $36 \text{ \AA}$  thick Fe and  $40 \text{ \AA}$  thick Si layers as a function of temperature (solid line). The upper curve was obtained by heating the sample at  $10^\circ\text{C}/\text{min}$  and subtracting a subsequent run on the same sample obtained under identical conditions. The baseline is the difference between the heat-flow rates of the second and third heating of the same sample. The sharp peak at  $500^\circ\text{C}$  comes from the heat evolved when the sample crystallized. The samples used in these studies were all annealed at temperatures below this peak temperature.

up to 500 °C. Beyond this temperature, the x-ray results indicated that the samples contained crystalline FeSi<sub>2</sub>. Thus, we attribute the broad low-temperature exotherm to the mixing of the Fe and Si layers and the sharp high-temperature isotherm to the formation of crystalline FeSi<sub>2</sub>. All of the samples discussed in this paper fall within the broad low-temperature peak region where the samples have an amorphous structure.

Annealed and unannealed samples were patterned into an eight terminal configuration that provided enough contacts for low-temperature conductance and Hall measurements. AZ1512 photoresist served as an etch mask, and a mixture of 10% HF + 20% HNO<sub>3</sub> + 70% H<sub>2</sub>O served as a sample etchant. In the processing of the photoresist it was necessary to heat the sample to 80 °C for 30 min. While there must be some interdiffusion of the Fe and Si layers during this step, our differential scanning calorimetry measurements indicate that it is negligible compared to that incurred by the thermal annealing steps described above.

The conductance measurements were performed using standard low level ac techniques. Care was taken to ensure that the measured conductances were independent of voltage for the voltages used in these experiments. The measurements were performed over a temperature range from 1.2 K <  $T$  < 20 K in a pumped helium cryostat and a gas flow cryostat. Temperatures were measured using a calibrated carbon glass resistor that was in intimate thermal contact with the sample.

### III. THEORETICAL BACKGROUND

Much recent experimental and theoretical work has shown that the conductivity of disordered metals decreases with temperature at temperatures that are low enough that electron-impurity scattering rates are greater than all other electron scattering rates. The functional form of this temperature dependence is determined by the dimensionality of the electronic system. It has been shown that for weakly disordered systems,  $k_F l > 1$ , there are two contributions to this temperature dependence.<sup>1-3</sup> The first arises from the weak localization of the electronic wave functions due to phase coherent backscattering effects. These WL corrections are very sensitive to processes that destroy the phase coherence of the electronic states.<sup>3</sup> The second contribution stems from the enhancement of electron-electron interactions that occurs in disordered metals. In contrast to the WL effects, these effects are insensitive (in most circumstances) to processes that break the phase coherence of the electronic states.<sup>1</sup> The total correction to the conductance as a function of temperature and magnetic field in two dimensional systems is<sup>1,3</sup>

$$G(T) - G(T_0) = \left[ \frac{e^2}{4\pi^2 \hbar} \right] A \ln \left( \frac{T}{T_0} \right), \quad (1)$$

where  $A = \alpha p + 1 - 3/4F$ .  $\alpha p$  comes from WL effects and  $1 - 3/4F$  comes from  $e-e$  interaction effects.  $\alpha$  is a constant of order 1 and  $F$  is a screening constant that

satisfies  $0 < F < 1$ . The constant  $p$  determines the temperature dependence of the electron phase coherence time for which we have assumed the form  $\tau_\phi \sim T^{-p}$ .<sup>14</sup> In three dimensional systems, the correction to the conductivity  $\sigma(T)$  follows<sup>1,16</sup>

$$\sigma(T) = \frac{e^2}{4\pi^2 \hbar} \left[ \frac{4}{3} - F \right] \left( \frac{k_B T}{\hbar D} \right)^{1/2}, \quad (2)$$

where  $D$  is the electronic diffusivity.

A crossover from two to three dimensional behavior for the  $e-e$  interaction contribution occurs when the film thickness exceeds the thermal diffusion length,  $L_T = \sqrt{\hbar D / k_B T}$ .<sup>1</sup> The WL contribution crosses over when the film thickness exceeds the electron phase coherence length,  $L_\phi = \sqrt{D \tau_\phi}$ .<sup>3</sup>

### IV. EXPERIMENTAL RESULTS

In Figs. 3(a) and 3(b) we have plotted the sheet conductance of two multilayers, one with 10 Å Fe and 32 Å Si layers (sample 1) and one with 10 Å Fe and 40 Å Si layers (sample 2), as a function of the logarithm of the temperature for different annealing temperatures. The conductances at 4.2 K for the two multilayers in the unannealed state are within 20% of one another and both show a logarithmic temperature dependence with  $A \simeq 20$ . This indicates that in their unannealed states the two films have nearly identical electrical characteristics and the temperature dependence of the conductance is dominated by two dimensional effects.

The responses of these samples to "low-temperature" anneals  $T_{\text{ann}} < 250$  °C are very similar. As shown in Fig. 4, the conductances of these samples at 4.2 K decrease with  $T_{\text{ann}}$  at the same rate. In addition, the  $G(T)$  fit the logarithmic form at the lowest temperatures throughout this regime. The slopes of the logarithmic fits to  $G(T)$ ,  $A$ , increase with annealing temperature at rates that are roughly the same for both samples. This is shown in Fig. 5, where we have plotted these slopes divided by the number of layers. For comparison, in Fig. 3(c), we plot the conductance as a function of temperature for the single layer sample annealed at different temperatures. Because this sample is so thin we expect that it remains two dimensional through all annealing steps. Like the multilayers, its conductance decreases with annealing and  $G(T)$  is logarithmic. Also, the slope of the logarithm increases with annealing. The similarities between this single layer behavior and the multilayer behavior give us confidence that these general effects are independent of the multilayer structure.

For  $T_{\text{ann}} > 250$  °C the responses of the two films diverge.  $G(4.2 \text{ K})$  of sample 2 drops less rapidly than for sample 1 and in fact it rises very rapidly (by a factor of 5) for  $T_{\text{ann}} > 300$  °C. Similarly, the measured values of  $A$  start to diverge near 250 °C. Finally, we show in Fig. 6 that  $G(T)$  for sample 2 after the 350 °C anneal fits a square root dependence better than a logarithmic dependence.

## V. DISCUSSION

## A. Overview

We present our discussion of the data in three sections. In the first two sections we separate the data into low  $T_{\text{ann}} < 250^\circ\text{C}$ , and high  $T_{\text{ann}} \geq 250^\circ\text{C}$  annealing temperature regimes. In the low  $T_{\text{ann}}$  regime, the two multilayers and the single layer samples show qualitatively similar behavior while in the high  $T_{\text{ann}}$  regime the behaviors of the two multilayers diverge. In the third section, we discuss possible explanations for the behavior of  $A$  with annealing temperature.

B. Data for  $T_{\text{ann}} < 250^\circ\text{C}$ 

The logarithmic temperature dependence of  $G(T)$  in both *unannealed* samples is characteristic of weak localization and disorder enhanced electron-electron interaction corrections to  $G(T)$  in two dimensional systems.<sup>1,2</sup> Given the ferromagnetic properties of the Fe layers<sup>12,13,17</sup> it is likely that the corrections to the conductance due to weak localization effects are strongly suppressed ( $\alpha p = 0$ ) and those due to electron-electron interaction effects are dominant. If the electrons are confined to individual layers in the unannealed multilayers then the  $A$  in Eq. (1) corresponds to  $20(1 - \frac{3}{4}F)$  for a 20 layer film. Thus, for

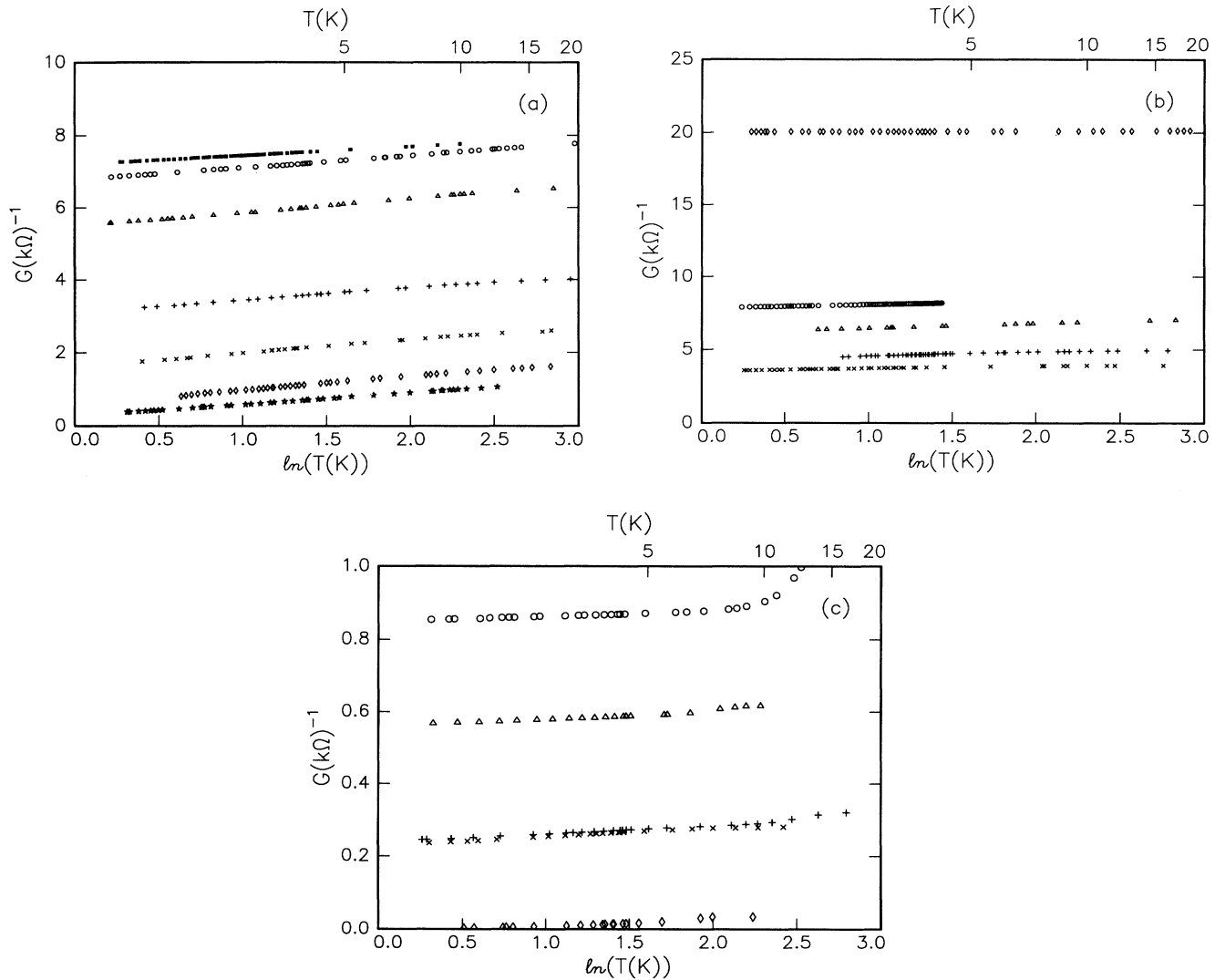


FIG. 3. (a) Sheet conductance versus  $\ln[T(K)]$  for sample 2:  $d_{\text{Si}} = 40 \text{ \AA}$ ,  $d_{\text{Fe}} = 10 \text{ \AA}$ . +, unannealed; o,  $150^\circ\text{C}$ ;  $\Delta$ ,  $200^\circ\text{C}$ ; +,  $250^\circ\text{C}$ ;  $\times$ ,  $300^\circ\text{C}$ ;  $\diamond$ ,  $350^\circ\text{C}$ ; \*,  $400^\circ\text{C}$ . (b) Sheet conductance versus  $\ln[T(K)]$  for Sample 1:  $d_{\text{Si}} = 32 \text{ \AA}$ ,  $d_{\text{Fe}} = 10 \text{ \AA}$ . +, unannealed;  $\Delta$ ,  $180^\circ\text{C}$ ; +,  $250^\circ\text{C}$ ;  $\times$ ,  $300^\circ\text{C}$ ;  $\diamond$ ,  $350^\circ\text{C}$ . Note that  $G(T)$  increases in the  $350^\circ\text{C}$  annealing step. (c) Sheet conductance versus  $\ln[T(K)]$  for the single layer sample. Si  $20 \text{ \AA}$ , Fe  $10 \text{ \AA}$ , Si  $20 \text{ \AA}$ . +, unannealed; o,  $150^\circ\text{C}$ ;  $\Delta$ ,  $200^\circ\text{C}$ ; +,  $250^\circ\text{C}$ ;  $\times$ ,  $300^\circ\text{C}$ .

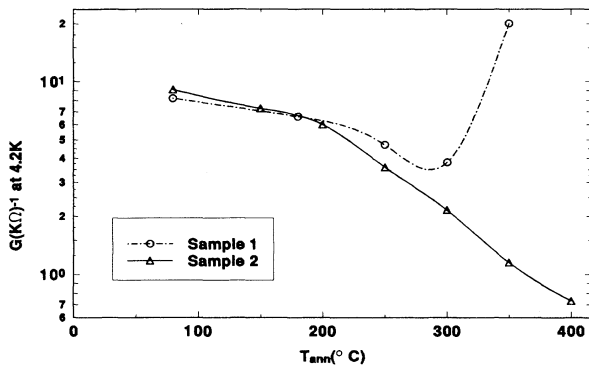


FIG. 4. Sheet conductance measured at 4.2 K versus annealing temperature for sample 1 and sample 2.

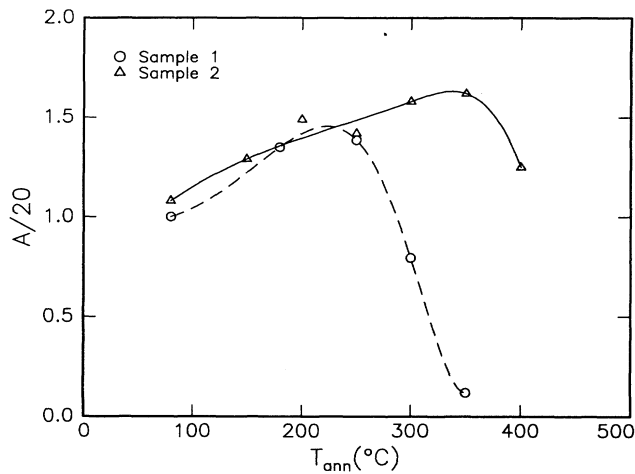


FIG. 5. Slopes of linear fits to the low-temperature data of Figs. 1(a) and 1(b). The slope is expressed in units of  $e^2/2\pi\hbar^2$  per layer.

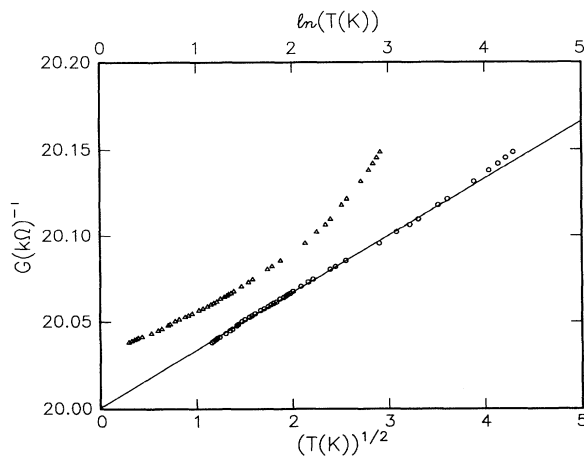


FIG. 6. Sheet conductance plotted versus  $\ln(T)$  and  $T^{1/2}$  for the multilayer sample with thinner Si layers after a 350 °C anneal.

the unannealed films  $F \approx 0$ . This is in agreement with earlier measurements on single ultrathin layers of Fe on Sb.<sup>20</sup> The fact that these samples show this dependence indicates that the conduction electrons are confined to individual Fe layers on the time scales relevant for weak localization or disorder enhanced electron-electron interaction effects. In short, the Fe layers in the unannealed multilayer films behave like independent two dimensional films. Their temperature dependent conductances add in parallel to give the multilayers conductance.

The decrease in conductance at 4.2 K in the initial stages of annealing of the two samples can be understood in terms of the bulk properties of solutions of  $\text{Fe}_x\text{Si}_{1-x}$ .<sup>18,19</sup> Earlier work on these amorphous composites showed that their room temperature resistivity increases with increasing amounts of Si.<sup>18,19</sup> Similar behavior has been observed in  $\text{Nb}_x\text{Si}_{1-x}$  composites which exhibit a metal to insulator transition at  $x = 11.5\%$ .<sup>20</sup> X-ray studies of the Fe/Si multilayers used in these experiments and other similar ones<sup>8</sup> show that annealing the multilayers leads to the interdiffusion of the Fe and Si layers. Consequently, the Fe in the conducting layers becomes diluted with Si and the layer conductances drop. This process of dilution of the Fe by the Si continues until the annealing temperature is high enough that crystallization of the Fe/Si film occurs at  $T_{\text{ann}} \approx 500^\circ\text{C}$  (see Fig. 2).

### C. Data for $T_{\text{ann}} \geq 250^\circ\text{C}$

We attribute the different behaviors of  $G$  with annealing at  $T_{\text{ann}} \geq 250^\circ\text{C}$  to the occurrence of a dimensional crossover from two dimensional (2D) to 3D electronic behavior in sample 1 that does not occur in sample 2. As shown in Fig. 2,  $G(T)$  is logarithmic for sample 2 up to the highest annealing temperatures and up to  $T_{\text{ann}} = 300^\circ\text{C}$  for sample 1 indicating that  $G(T)$  is dominated by two dimensional effects in these regimes. The change in  $G(T)$  to a square root temperature dependence in sample 1 after a 350 °C anneal is consistent with a crossover from two to three dimensional electron transport [see Eq. (2)]. The resistivity at 4.2 K of this sample after the 350 °C anneal is 4000  $\mu\Omega\text{ cm}$ . Using Eq. (2) and the slope of the square root temperature dependence we find that  $D = 3.7 \times 10^{-4} \text{ m}^2 \text{ sec}^{-1}$  if we assume that  $F = 0$ . Using this value for  $D$  and the measured value for the resistivity we can calculate the density of states at the Fermi energy within a free electron model. We find that  $N(E_F) = 1.7 \times 10^{21} / \text{cm}^3 \text{ V}$ . These values for  $D$  and  $N(E_F)$  are reasonable for an amorphous composite material and give us further confidence that the change in the temperature dependence of the conductivity stems from a dimensional crossover effect.

The divergence of the dependence of  $G(4.2 \text{ K})$  on  $T_{\text{ann}}$  for the two multilayers and, in particular, the sharp increase in  $G(4.2 \text{ K})$  that occurs at 350 °C in sample 1 also points to the occurrence of a dimensional crossover in it. As shown in Fig. 5,  $G(4.2 \text{ K})$  for sample 2 decreases monotonically up to the highest annealing temperature of 400 °C. This suggests that the process described in the

preceding section continues and dominates the behavior of sample 2 up to the highest annealing temperatures. This process, however, cannot account for the slowing down of the decrease and subsequent rise in  $G(4.2\text{ K})$  for sample 1. We attribute this behavior to the fact that  $e$ - $e$  interaction and weak localization effects are stronger in two dimensions than in three dimensions.<sup>1-3,21</sup> When the dimensional crossover occurs the suppression of the conductivity by these effects becomes reduced and the conductivity rises. Since each layer of these films has a very high sheet resistance prior to the last two annealing steps  $R \simeq 4\text{ k}\Omega$ , the conductivity rise is dramatic.

The occurrence of this dimensional crossover implies that the electronic coupling between the conducting layers grows as the multilayers are annealed. In a simple model, the rate at which electrons move between conducting layers depends on the conductivity and thickness of the intervening, more Si rich layers. As Fe diffuses into these layers during the annealing process, their conductivity rises and their effective thicknesses change in such a way that this rate increases. A dimensional crossover occurs in sample 1 because this rate eventually becomes large enough that the electrons move among layers on time scales shorter than those relevant to  $e$ - $e$  interaction effects.

It may seem surprising that a difference of only  $8\text{ \AA}$  in the Si layer thicknesses of samples 1 and 2 can give rise to a dimensional crossover in one and not the other. We assert that this extreme sensitivity to the Si layer thickness comes about because these samples have total Fe concentrations that are very near the critical value for the 3D metal to insulator transition. Referring to Fig. 1, we envision that the concentration profiles of multilayers in the high annealing temperature regime qualitatively mimic the ‘‘annealed’’ curve. If the concentration in the Si rich parts of the layer is below the critical concentration of the metal-insulator transition  $x_c$ , then these regions will have nearly zero conductivity and the coupling between the Fe rich layers will be weak. If, on the other hand, the concentration of the Si rich parts exceeds  $x_c$ , then the conductivity will be finite and the coupling between the Fe rich layers will be strong. This makes the coupling of the conducting layers through the nonconducting layers a very sensitive function of concentration when the total concentration of the sample is near  $x_c$ . Our estimate of  $x_c \simeq 30\%$  indicates that we are in this concentration regime.

To summarize, the interdiffusion of the Fe and Si reduces the conductivity of the Fe layers by reducing the Fe concentration in them and it also causes an increased interlayer coupling that leads to a dimensional crossover that increases the conductivity. Above  $T_{\text{ann}} = 350^\circ\text{C}$ , the latter effect predominates.<sup>1</sup>

#### D. Changes in $A$ with annealing

A further interesting aspect of these data is the behavior of  $A$  upon annealing. Normally, ultrathin films that contain a high density of magnetic moments do not show WL effects in the conductivity, i.e.,  $\alpha p = 0$  in Eq. (1).

This is because either spin-flip or skew scattering of the conduction electrons from the magnetic moments or local magnetic field effects determine  $L_\phi$ . These effects are usually temperature independent and therefore,  $\alpha p = 0$  in Eq. (1). Thus, we expect that  $A \leq 1$ , since theoretically,  $0 \leq F \leq 1$ .<sup>1</sup> As shown in Fig. 5, however,  $A$  rises above 1. As an explanation for this discrepancy, we suggest that annealing weakens the magnetic properties of these films and in effect, ‘‘turns on’’ the WL contributions to the conductance. The interdiffusion of Fe and Si driven by annealing probably leads to the disappearance of the permanent magnetic properties of the films (see discussion in Sec. II). In addition, as the Fe and Si interdiffuse the magnetic moments of the individual Fe atoms may weaken and disappear due to the appearance of crystal field effects from the Si atoms surrounding the Fe atoms or the hybridization of the Fe  $d$  levels with the  $sp$  levels of the surrounding Si. Thus, if the WL effects are destroyed in the as-deposited films by ‘‘magnetic’’ effects, then it seems reasonable that they should appear with annealing. To determine whether this picture is correct further magnetoresistance studies to determine the temperature dependence and strength of the electron phase breaking rates would be illuminating.

As shown in Fig. 5,  $A$  does start to decrease in sample 1 for  $T_{\text{ann}} > 300^\circ\text{C}$ . Earlier work on Si/Au multilayers suggests that this behavior is caused by the growth of interlayer coupling.<sup>7</sup>

## VI. SUMMARY

We have presented measurements of the conductance as a function of temperature of amorphous Fe and Si multilayers as a function of the temperature at which they are annealed. At low annealing temperatures,  $T_{\text{ann}} < 250^\circ\text{C}$ , the conductances of the samples decrease as the Fe and Si layers interdiffuse and the concentration of the Fe layers decreases toward the metal-insulator transition value. The temperature dependence of the conductance of these films assumes the form expected for disordered metal films in the two dimensional limit. At higher annealing temperatures  $T_{\text{ann}} > 250^\circ\text{C}$  the conductance of samples with relatively thick Si layers continues to drop and the two dimensional temperature dependence persists. In contrast, the conductance of a sample with relatively thin Si layers increases sharply and changes to a three dimensional temperature dependence at the highest annealing temperatures. We have attributed these different behaviors to the occurrence of a dimensional crossover in the latter sample that does not occur in the former.

## ACKNOWLEDGMENTS

We have benefitted from discussions with D. Belitz. This work was supported primarily by NSF Grant DMR-9122268 at Brown University and by the Office of Naval

Research Grant (No. N001-91-J-1288) and National Science Foundation Grant No. DMR-9213352 at the University of Oregon. Additional support was provided by the Murdock Foundation. Thomas Novet gratefully ac-

knowledges support from the U.S. Department of Education Graduate Assistance in Areas of National Need program (No. P200A10238). J.M.V., Jr. acknowledges support from the Alfred P. Sloan Foundation.

- 
- <sup>1</sup> B.L. Altshuler and A.G. Aronov, *Electron-electron Interactions in Disordered Systems*, edited by A. L. Efros and M. Pollak (Amsterdam, Oxford, 1985), p. 1.
- <sup>2</sup> R.C. Dynes and P.A. Lee, *Science* **223**, 355 (1984).
- <sup>3</sup> G. Bergmann, *Phys. Rep.* **107**, 1 (1984).
- <sup>4</sup> W.L. McMillan, *Phys. Rev. B* **24**, 2739 (1980); D. Belitz and T.R. Kirkpatrick, *Rev. Mod. Phys.* (to be published).
- <sup>5</sup> D. Neerincx, K. Temst, M. Baeert, E. Osquiguil, C. Haesendonck, Y. Bruynseraede, A. Gilabert, and I.K. Schuller, *Phys. Rev. Lett.* **67**, 2577 (1991).
- <sup>6</sup> B.Y. Jin and J.B. Ketterson, *Phys. Rev. B* **33**, 8797 (1986); B.Y. Jin, Y.H. Shen, and H.Q. Yang, *Superlatt. Microstruct.* **1**, 401 (1985).
- <sup>7</sup> N. Cherradi, A. Audouard, G. Marchal, J.M. Broto, and A. Fert, *Phys. Rev. B* **39**, 7424 (1989).
- <sup>8</sup> Thomas R. Novet and David C. Johnson, *J. Am. Chem. Soc.* **113**, 3398 (1991); Thomas R. Novet, David C. Johnson, and John M. McConnell, *Chem. Mater.* **4**, 473 (1992).
- <sup>9</sup> A. Langenfeld and P. Wölffe, *Phys. Rev. Lett.* **67**, 739 (1991).
- <sup>10</sup> Y.K. Lin, T.R. Novet, D.C. Johnson, and J.M. Valles, Jr. (unpublished).
- <sup>11</sup> P. Mangin, M. Piecuch, G. Marchal, and C. Janet, *J. Phys. F* **8**, 2085 (1978).
- <sup>12</sup> C. Dufour, A. Bruson, G. Marchal, B. George, and P. Mangin, *J. Magn. Mater.* **93**, 545 (1991).
- <sup>13</sup> X.D. Ma, Y.H. Liu, and L.M. Mei, *J. Phys. Condens. Matter* **3**, 7139 (1991).
- <sup>14</sup> We assume  $\tau_\phi \sim T^{-p}$ , and realize that it is restrictive. For example, there can be interesting magnetic scattering effects that do not have this temperature dependence (Ref. 15). These effects would not contribute a logarithmic temperature dependence to  $G(T)$ . Since this is the primary dependence that we observe, we conclude that such effects do not significantly affect  $G(T)$  in our multilayers.
- <sup>15</sup> B. Barbara, V.S. Amaral, J. Filippi, A.G.M. Jansen, J.B. Sousa, and J.M. Moreira, *J. Appl. Phys.* **70**, 5813 (1991).
- <sup>16</sup> D.S. Maclachlan, *Phys. Rev. B* **28**, 6821 (1983).
- <sup>17</sup> G. Bergmann and F. Ye, *Phys. Rev. Lett.* **67**, 735 (1991).
- <sup>18</sup> T. Lucinski and J. Baszynski, *Phys. Status Solidi* **84**, 607 (1984); T. Lucinski and B. Szymanski, *ibid.* **96**, K53 (1986).
- <sup>19</sup> Y. Shimada and H. Kojima, *J. Appl. Phys.* **49**, 932 (1978).
- <sup>20</sup> D.J. Bishop, E.G. Spencer, and R.C. Dynes, *Solid State Electron.* **28**, 73 (1985); G. Hertel *et al.*, *Phys. Rev. Lett.* **50**, 743 (1983).
- <sup>21</sup> We do not believe that this jump stems from a change in the mean free path of the electrons. Before and after the 350 °C annealing step the samples are amorphous so that the mean free path remains the order of an interatomic spacing throughout the annealing processes.